공학석사학위논문

Bioabsorbable bone plate with a radiopaque layer containing barium sulfate for diagnostic X-ray imaging

진단용 X-선 영상을 위한 황산바륨 조영층이 결합된 생체흡수성 골 고정용 플레이트의 개발

2014 년 2 월

서울대학교 대학원

협동과정 바이오엔지니어링전공

최 성 윤

Bioabsorbable bone plate with a radiopaque layer containing barium sulfate for diagnostic X-ray imaging

진단용 X-선 영상을 위한 황산바륨 조영층이 결합된 생체흡수성 골 고정용 플레이트의 개발

지도교수 최 영 빈

이 논문을 공학석사 학위논문으로 제출함

2013 년 12 월

서울대학교 대학원

협동과정 바이오엔지니어링전공

최 성 윤

최성윤의 석사 학위논문을 인준함

2014 년 2 월

위 원 장 _____ (인)

부위원장 _____ (인)

위 원 _____ (인)

Abstract

Bioabsorbable bone plate with a radiopaque layer containing barium sulfate for diagnostic X-ray imaging

Sung Yoon Choi

Interdisciplinary Program in Bioengineering, College of Engineering,

The Graduate School

Seoul National University

Bone fixation systems made of biodegradable polymers are radiolucent, making post-operative diagnosis with X-ray imaging a challenge. In this study, to allow X-ray visibility, we separately prepared a radiopaque layer and attached it to a bioabsorbable bone plate approved for clinical use (Inion, Finland). We employed barium sulfate ($BaSO_4$) as a radiopaque material due to the high X-ray attenuation coefficient of barium (2.196 cm^2/g). The radiopaque layer was composed of a fine powder of $BaSO_4$ bound to a biodegradable material, poly (lactic-co-glycolic acid) (PLGA), to allow layer degradation similar to the original Inion bone plate. In this study, we varied the mass ratio of $BaSO_4$ and PLGA in the layer to be 3:1 w/w or 10:1 w/w to modulate the degree and longevity of X-ray visibility. All radiopaque plates

herein were visible *via* X-ray, both *in vitro* and *in vivo*, for up to 40 days. The radio-opacity increased with increasing $BaSO_4$ content. For all layer types, the radio-opacity decreased with time due to the swelling and degradation of PLGA, and the change in the layer shape was more apparent for layers with the higher PLGA content ($BaSO_4$: PLGA = 3:1 w/w). The radiopaque plates released, at most, 0.5 mg of $BaSO_4$ every two days in a simulated *in vitro* environment, for which cytotoxicity did not appear. The radiopaque plates also exhibited good biocompatibility, similar to that of the Inion plate, 1 and 4 months following implantation. Therefore, we concluded that the $BaSO_4$-based radiopaque, biodegradable plate prepared in this work has the potential to be used as a fixation device with both X-ray visibility and biocompatibility.

Keywords: Barium sulfate; biocompatibility; biodegradation; fixation system; poly (lactic-*co*-glycolic acid); X-ray visibility

Student Number: 2012-21022

Contents

List of Figures

List of Tables

Ⅰ. Introduction

1.1. *Biodegradable bone fixation systems*

Bone fixation systems, i.e., bone plates and screws, have been widely used for orthopedic treatments of bone fracture and reconstruction in clinical practice [1, 2]. The plate is positioned on the fractured bone and fixed by screws to hinder undesired motion until healing is complete. Thus, the majority of fixation devices are composed of a rigid material, such as metal, to support mechanical loads on fractured bone [3, 4]. However, this non-degradable system often leads to bone resorption due to stress shielding, thereby impeding bone growth [5]. Bone fixation systems can also interfere with bone growth in children following the healing of the fracture [6]. Therefore, non-degradable, metallic fixation systems often require a secondary removal surgery.

In this context, biodegradable bone plates and screws have attracted significant attention [7-10]. Biodegradable fixation systems can be used to replace metallic systems, especially when high mechanical loads are not applied to the treatment area. Because they are biodegradable, these systems gradually decrease in strength, allowing stress to be shifted to the bone and enabling dense bone formation [11-13]. Biodegradable fixation systems are primarily composed of biodegradable polymers, such as poly (lactic acid) (PLA) and poly

(glycolic acid) (PGA) [14, 15], which are known to degrade by hydrolysis and be metabolized in the human body [16-18].

Proper positioning and fixation of the plate is critical for the treatment of a bone fracture because plate loosening can result in a gap at the fracture, hindering healing and leading to infection [19]. This complication can often be diagnosed *via* X-ray imaging in clinical practice [20, 21], which is easily performed for metallic systems due to their inherent radio-opacity. However, biodegradable fixation systems are not visible *via* X-ray due to the radiolucency of the composing materials, *i.e.*, biodegradable polymers [22-24]. Furthermore, changes in the proper positioning of the plate can be a serious problem if they are not detected in a timely manner.

1.2. *Radiopaque functionality with barium sulfate*

Previously, to allow X-ray visibility, we prepared and attached a radiopaque layer to a biodegradable bone plate already in clinical use [25]. The layer comprised β-tricalcium phosphate (TCP) and poly(lactic-*co*-glycolic acid) (PLGA) as a radiopaque material and biodegradable polymeric binder, respectively. With this material, the positioning of the plate could be monitored *via* X-ray for a period of clinical need, and the layer was also able to gradually degrade without compromising the biocompatibility of the original bone plate. However, the discernibility of the layer *via* X-ray imaging *in vivo* was not satisfactory due to the relatively low X-ray attenuation coefficient of calcium in TCP.

To address this shortcoming, we suggest barium sulfate ($BaSO_4$) as an alternative material for preparing radiopaque layers, as barium is known to possess an X-ray attenuation coefficient (2.196 cm^2/g) much larger than that of calcium (0.2571 cm^2/g) [26]. Due to its high X-ray absorption, $BaSO_4$ has previously been used as a radiopaque material to allow monitoring of the position of implanted medical devices in clinical use, such as vertebroplasty cements and endodontic sealers [27-29]. Despite its advantages, there was concern that $BaSO_4$ might be toxic inside the body [30]. For this reason, $BaSO_4$ is generally contained and sealed to prevent its release from the implantable devices in clinical use [27-29].

In this work, therefore, we aimed to prepare a radiopaque bone plate containing $BaSO_4$ for enhanced X-ray visibility, while also adjusting $BaSO_4$ release to avoid and minimize the possibility of toxicity caused by $BaSO_4$. We again separately prepared a radiopaque layer made of a mixture of $BaSO_4$ and a binder material, PLGA, and attached it to a biodegradable bone plate in clinical use, as in our previous work [25]. To control the release of $BaSO_4$, we varied the mass ratio of $BaSO_4$ to PLGA in the layer. In this way, the $BaSO_4$ content in the layer changed with time depending on the incorporated amount of PLGA. Thus, the longevity of the X-ray visibility could be tailored.

1.3. *Characterization of radiopaque layered bone plates*

The radiopaque plates containing $BaSO_4$ were characterized using scanning electron microscopy (SEM), Fourier transform infrared spectroscopy (FTIR) and X-ray diffraction (XRD). We performed an *in vitro* immersion test in a simulated biological fluid to examine the change in X-ray visibility of the radiopaque plates with time, and the released barium ions were also quantitatively measured using inductively coupled plasma atomic emission spectroscopy (ICP-AES). To examine cytotoxicity, the plates were assessed using L929 mouse fibroblasts. For *in vivo* evaluation, the plates were fixed to the humerus bones of rabbits and imaged *via* X-ray at scheduled intervals for 56 days following implantation. For biocompatibility evaluation, the histopathologic analyses were performed using tissue samples around the plates obtained at 1 and 4 weeks after implantation.

Ⅱ. Materials and methods

2.1. *Materials*

Barium sulfate ($BaSO_4$) was obtained from Sigma-Aldrich (Missouri, USA), and poly (lactic-*co*-glycolic acid) (PLGA; average MW = 4.1 kDa; i.v. = 0.08 dL/g) was obtained from Lakeshore Biomaterials (Alabama, USA). Phosphate buffered saline (PBS, pH 7.4) was obtained from the Seoul National University Hospital Biomedical Research Institute. Dichloromethane (DCM) and dimethylformamide (DMF) were supplied from J.T. Baker (Pennsylvania, USA). Bioabsorbable bone fixation plates (PLT-1031) and screws (SCR-1222) were purchased from Inion (Finland). Zolazepam and tiletamine (0.2 ml/kg; Zoletil®) were supplied from Virbac (France) and xylazine (0.07 ml/kg; Rompun®) was from Bayer (Germany). Betadine® was obtained from Hyundai Pharm (Korea). The absorbable sutures (Vicryl 4-0) used for animal surgery were supplied from Ethicon (New Jersey, USA).

2.2. *Preparation of radiopaque layers*

We prepared our radiopaque layers following the method described in our previous study [25] but with slight modifications, as described in Figure 1. Briefly, we first cut a 0.5 mm-thick sheet of poly (methylmethacrylate) (PMMA) (GoodFellow, England) to form a square-frame shape with an outer edge of 6.0 mm and a concentric

square hole with sides of 1.0 mm using a CO_2 laser (FC-200RA LASER Machinery, South Korea). The resulting sheet then served as a mold to prepare a substrate made of polydimethylsiloxane (PDMS) (Sylgard®184, Dow Corning, Michigan, USA). The wells on the PDMS substrate were then used as a mold for the radiopaque layers.

We prepared two distinct types of radiopaque layers comprising mass ratios of $BaSO_4$ to PLGA of either 10:1 w/w or 3:1 w/w to give 10BFL and 3BFL, respectively. Both layers were prepared in a 0.5 mm in thickness. To prepare 10BFL or 3BFL, a fine powder of 400 mg $BaSO_4$ was added to 100 μl of a 40 % w/v PLGA solution or 148 μl of a 90 % w/v PLGA solution in DMF, respectively. The mixture was then filled in the PDMS mold with a doctor-blade method and freeze-dried for 1 day. The dried mixture was then removed from the PDMS mold to give the radiopaque layer used in this work.

2.3. *Preparation of radiopaque bone plates*

To provide X-ray visibility, we physically attached a radiopaque layer to a bioabsorbable bone plate in clinical use (PLT-1031, Inion, Finland). We first cut a whole piece of an Inion bone plate into a 6.5 mm x 6.5 mm square-shaped piece with a screw hole at the center. To attach the radiopaque layer, we sprayed a 30 % w/v PLGA in DCM solution on the surface of the resulting piece of a bone plate under the following conditions: diameter of nozzle orifice, 0.5 mm; spraying pressure, 15 psi; spraying time, 2 s; and distance from sample to nozzle, 15 cm. The radiopaque layer was then immediately placed and pressed on top of

the bone plate. The resulting radiopaque plate was then lyophilized for over 1 day to remove residual DCM. In this work, using two different compositions of radiopaque layers, we fabricated two different types of radiopaque plates: plates attached with either 3BFL or 10BFL resulting in 3BFL and 10BFL plates, respectively.

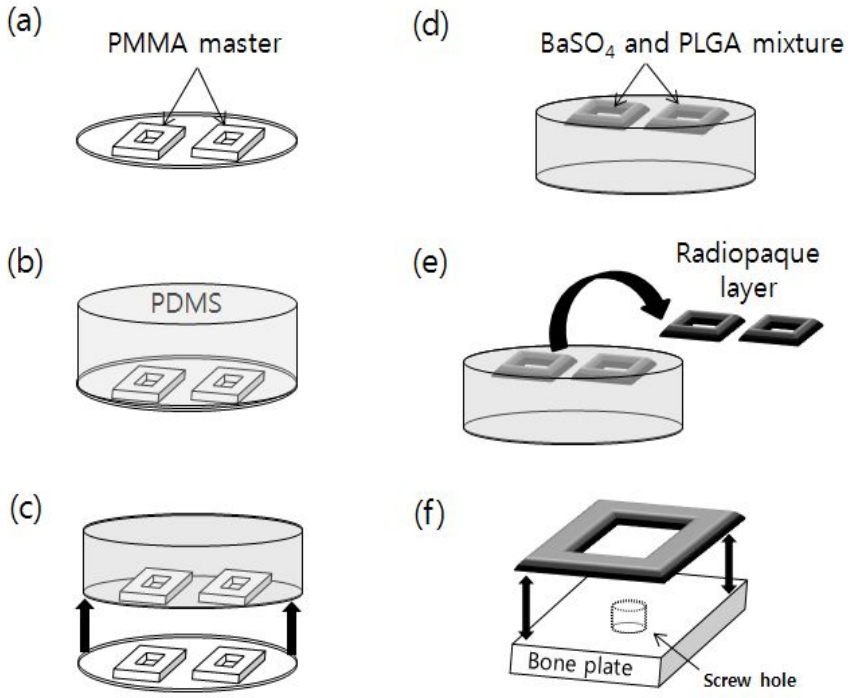

Figure 1. Schematic process for preparation of the radiopaque plates.

2.4. *Characterization of radiopaque layers*

To examine the layer morphology, the $BaSO_4$ particles and the radiopaque layers were imaged by SEM (7401F, Jeol, Japan). Prior to imaging, the samples were sputter-coated with platinum for 10 min (208HR, Cressington Scientific, England). The XRD patterns of the radiopaque layers were obtained using an X-ray diffractometer (D/MAX RINT 2200-Ultima, Rigaku, Japan) equipped with Ni-filtered Cu-K_α radiation (λ=1.5418 Å), where the operation voltage and current were set at 40 kV and 30 mA, respectively. The samples were continuously scanned in the 2θ range at 10 º – 70 º with a step size of 0.02 º. We also performed Fourier transform infrared spectroscopy (FTIR; JASCO 6100, Japan) to assess the composition of the radiopaque layers using the KBr pellet technique.

2.5. *In vitro X-ray visibility test*

To examine the longevity of the X-ray visibility, the radiopaque plates prepared in this work were each immersed in 10 ml of simulated biological fluid (PBS, pH 7.4) and then placed in a shaking incubator (SI-600R, Jeio Tech, Korea) at 125 rpm and 37 ºC. At scheduled intervals, the plates were imaged with a mobile C-arm (BV pulsera, Philips, Netherlands) in manual mode with a charging voltage of 55 kV.

The images were obtained with a 1024 x 1024 pixel resolution, where the contrast was automatically managed with built-in software (HQ Orthopedic mode). More than three samples were assessed for each type of radiopaque plate (10BFL or 3BFL plates). The images

were then analyzed by densitometry using Image J software (National Institutes of Health, USA). For each X-ray image, the average densitometry value was obtained from at least 300 pixels within the visible area of the radiopaque plate and subsequently subtracted by the background value measured from the area outside of the plate.

2.6. *Cytotoxicity evaluation*

We used the L929 mouse fibroblast cell line (Korean Cell Line Bank, Korea) to assess the cytotoxicity of the radiopaque plates prepared in this work. For cell cultivation, we used a RPMI-1640 medium (WelGENE, Korea) supplemented with 10 % fetal bovine serum (Gibco, Life Technologies, UK) and 1 % antibiotics (penicillin, 10,000 U ml^{-1} and streptomycin, 10,000 μg ml^{-1}; Gibco, Life Technologies, UK).

We performed the extraction method following the ISO 10993-5 standard guidelines [31] to examine the cytotoxic effect of the released $BaSO_4$ particles from the radiopaque plates. The intact 10BFL and 3BFL plates were each placed in 2 ml of immersion medium (the same medium used for cell culture) and incubated with continuous agitation (125 rpm) at 37 ºC (SI-600R, Jeio Tech, Korea). All plates were sterilized prior to the test using ethylene oxide gas. Every two days, the entire 2 ml of immersion medium was withdrawn to provide the extract medium, and an equal volume of the fresh medium was added. For both types of plates, the extract media were obtained on days 1, 3, 7, 14, 21, 30 and 42, for cytotoxicity evaluation.

The L929 fibroblasts were prepared at a density of 4 x 10^5 per well on a 96-well cluster cell culture plate, which was incubated in a humidified atmosphere with 5 % CO_2 at 37 ºC for 24 h (HERAcell 150i,Thermo Scientific, USA). Subsequently, 100 µl of the culture medium from each well was replaced with an equal volume of the extract medium obtained above. The medium containing 2 % Triton X-100 (Sigma-Aldrich, USA) and intact medium without treatment were used for positive and negative controls, respectively. After adding the extract medium, the cells were incubated for another 24 h. Following treatment, the cells were assayed with an *in vitro* toxicology assay kit, following the supplier's instructions (TOX1, Sigma Aldrich, MO, USA), 10 µl of 1 mg/ml MTT (tetrazolium salt 3-2,5-diphenyltetrazolium bromide) solution prepared in phosphate buffered saline (PBS, pH 7.4) was added to the wells that had been treated with various types of extraction media. After 4 h of incubation, the medium from each well was aspirated, and each well was then treated with 100 µl of the solubilization solution (10 % Triton X-100 in acidic isopropanol, 0.1 N HCl), which was measured spectrophotometrically with an ELISA reader (VersaMax ELISA Microplate Reader, Molecular Devices, CA, USA) at wavelengths of 570 nm (sample) and 690 nm (reference). At least five samples were tested for each sample time and each type of plate for statistical analysis.

2.7. *In vitro release test of $BaSO_4$ particles*

To examine the quantity of released $BaSO_4$ particles, the intact 10BFL and 3BFL plates were each placed into 2 ml of immersion medium (the same medium used for cell culture) and incubated with continuous agitation (125 rpm) at 37 ºC (SI-600R, Jeio Tech, Korea). Every two days, the entire 2 ml of immersion medium was withdrawn to provide the extract medium, and an equal volume of fresh medium was added. The extract media obtained on days 1, 7, 21, and 40 were used to measure the amount of released $BaSO_4$ particles.

The extract media samples were lyophilized to produce a dry powder containing $BaSO_4$, which was treated with 8 ml of solution of HNO_3, HF and $HClO_4$ (4:4:1 = v/v/v), followed by the addition of 8 ml of a different solution comprising HCl, HNO_3 and HF (9:3:4 = v/v/v), to fully dissolve the powder. The solution was then analyzed by ICP-AES (OPTIMA 4300DV, Perkin-Elmer, USA) to quantify the concentration of barium ions, which was then converted to the released amount of $BaSO_4$. For this analysis, the plasma in argon gas was created at a frequency of 40 MHz and a power level of 1.3 kW, and the detection wavelengths used were 167 – 782 nm.

2.8. *In vivo evaluation of radiopaque plates*

For the *in vivo* evaluation of the radiopaque plates, we used 12-week-old male New Zealand White (NZW) rabbits weighing 2.5 - 2.8 kg (Cheonan Yonam College, Chungcheongnam-do, Korea). The rabbits were individually housed and cared for following protocol approved by

the Institutional Animal Care and Use Committee (IACUC No. 11-0026) at Seoul National University Hospital. The rabbits were provided food and water without restriction.

We implanted and fixed each of the intact 3BFL and 10BFL plates on the humerus of the rabbits *in vivo*. The radiopaque plate with either a 3BFL or a 10BFL, was fixed on the right humerus, and an unmodified plate (i.e., an intact Inion plate without radio-opacity) was implanted on the left humerus to serve as a control. At least five animals were tested for each type of radiopaque plate prepared in this work to allow statistical analysis. For the fixation surgery, anesthesia was performed by intramuscular injection of a 20 mg/kg cocktail of Zoletil® and Rompun® (3:1 = v/v). Subsequently, the hair on the operation site was cleanly shaved and cleaned with Betadine®. The incision was made on the skin and the underlying muscle above the humerus, and the periosteum was incised to expose a sufficient area for plate fixation. The humerus was drilled with an electric drill (ADL-48, AIMSAK, Korea), followed by tapping with a manual tapper (IMS 9027, Inion, Finland) to prepare a screw hole in the bone. The plate was then fixed in place by a biodegradable screw (SCR-1222, Inion, Finland). The dissected periosteum, muscle, and skin were closed with absorbable sutures (Vicryl 4-0, Ethicon, New Jersey, USA). To prevent infection, a post-operative dressing was applied with Betadine®.

To evaluate X-ray visibility following the plate fixation *in vivo*, the humeri of the rabbits were imaged with a mobile C-arm (BV Pulsera, Philips, Netherlands) in manual mode with a charging voltage

of 55 kV. The images were obtained at scheduled periods of 4, 8, 16, 26, 36, 46, and 56 days following implantation to examine the longevity of the X-ray visibility of the plates. During imaging, the rabbits were under temporary anesthesia *via* intramuscular injection of a 20 mg/kg cocktail of Zoletil® and Rompun® (3:1 = v/v). The images were quantitatively analyzed by densitometry using Image J software (National Institutes of Health, Maryland, USA). For each X-ray image, the average densitometry value was measured over 300 pixels within the visible area of the radiopaque plate and subtracted by the average background value obtained from the area outside of the plate. We also evaluated the area of X-ray visibility. For this, the pixels over a 170 threshold value in grey scale were selected within the area inside of the radiopaque plate using the wand tool in the Image J software. The selected area was then expressed as a percentage of the entire area of the intact radiopaque layer (20 mm^2).

We also investigated the *in vivo* biocompatibility of the radiopaque plates prepared in this work. For this, the rabbits that underwent plate implantation were sacrificed by intravenous injection of potassium chloride (KCl, 10 ml) under deep anesthesia (1 ml/kg Zoletil®), and the tissues around the plates were biopsied at 1 and 4 weeks after implantation. The tissue samples were then embedded with resin and sectioned into 40 – 50 μm slides (BS-3000N, EXAKT, Germany), which were then stained with hematoxylin and eosin (H&E). The slides were examined under an optical microscope with x12.5 and

x400 magnifications (BX53F, OLYMPUS, Japan) for histopathologic evaluation by a professional pathologist.

The extent of inflammatory response was assessed semi-quantitatively based on the presence of neutrophils, lymphocytes, pigment-laden macrophages, new bone formation and fibrosis. The numbers of neutrophils, lymphocytes and the extent of new bone formation were graded as absent (0), mild (1), or moderate (2); the infiltration of pigment-laden macrophages as absent (0), mild (1), moderate (2), or marked (3); the extent of fibrosis as absent (0), limited to peri-implant soft tissue without extension to skeletal muscle (1), extended to skeletal muscle but not beyond it (2), or extended to fat tissue beyond skeletal muscle (3).

2.9. *Statistics*

A statistical analysis of the data from the cytotoxicity evaluation was performed using ANOVA with $\alpha = 0.05$ followed by pairwise comparisons using a Tukey's post hoc test (Statistical Package for the Social Sciences (SPSS), version 19, USA). An unpaired t-test was performed to compare the densitometry measurements between 10BFL and 3BFL, where $p < 0.05$ was considered statistically significant (*in vitro* densitometry: SPSS, version 19, USA; *in vivo* densitometry: GraphPad Prism 5, USA).

Ⅲ. Results

3.1. *Characterization of radiopaque layer*

In this work, to vary the degree of X-ray visibility and control the rate of layer degradation, we prepared two different radiopaque layers, 10BFL (PLGA: $BaSO_4$ = 1:10 w/w) and 3BFL (PLGA: $BaSO_4$ = 1:3 w/w). Figure 2(a) depicts an intact piece (6.5 mm X 6.5 mm) of the bioabsorbable bone plate (PLT-1031, Inion, Finland) used in this work. On top of this plate, we attached a radiopaque layer composed of PLGA and $BaSO_4$ (Fig. 2(b)). The layer was designed to possess a frame shape with a square hole at the center in order to leave the screw hole already present in the original bone plate unhindered. Under SEM observation, the $BaSO_4$ particles in the radiopaque layers were observed to be bound with PLGA, and the particle size was measured to be 1.58 ± 0.35 μm (Fig. 2(c)).

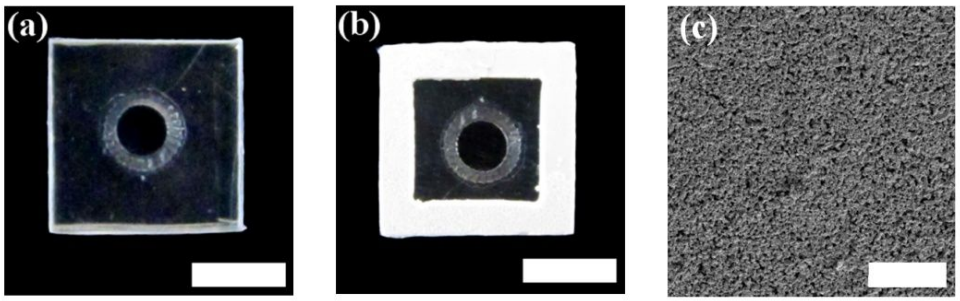

Figure 2. Optical images of the bone plates (a) without and (b) with a radiopaque layer. (c) Scanning electron micrograph of the surface of a radiopaque layer. The scale bars are (a-b) 3 mm and (c) 10 μm.

We performed XRD and FTIR analyses on the radiopaque layer. As displayed in Figure 3, the characteristic XRD peaks from the intact $BaSO_4$ powder [32] were also observed in both 10BFL and 3BFL.This result indicated the presence of crystalline $BaSO_4$ particles in the radiopaque layer. The intact PLGA exhibited no XRD peaks due to its amorphous structure [33]. As we examined in the FTIR spectra (Fig. 4), the intact $BaSO_4$ powder displayed characteristic peaks at 1073 – 1192 cm^{-1} and 610 – 638 cm^{-1} due to sulfate (SO_4^{2-}) vibrations [32]. The intact PLGA exhibited a strong band at 1758 cm^{-1} from the carbonyl group and bands at 2948 – 2998 cm^{-1} from the $–CH_2$ groups. The absorption bands at 1132 and 1186 cm^{-1} were ascribed to the C-O stretching of the ester group [33]. The characteristic peaks from both the intact $BaSO_4$ powder and the PLGA were observed to overlap with those from the radiopaque layers of 10BFL and 3BFL, revealing that the composing materials, $BaSO_4$ and PLGA, were physically mixed to form a rigid layer without changing their individual chemical properties.

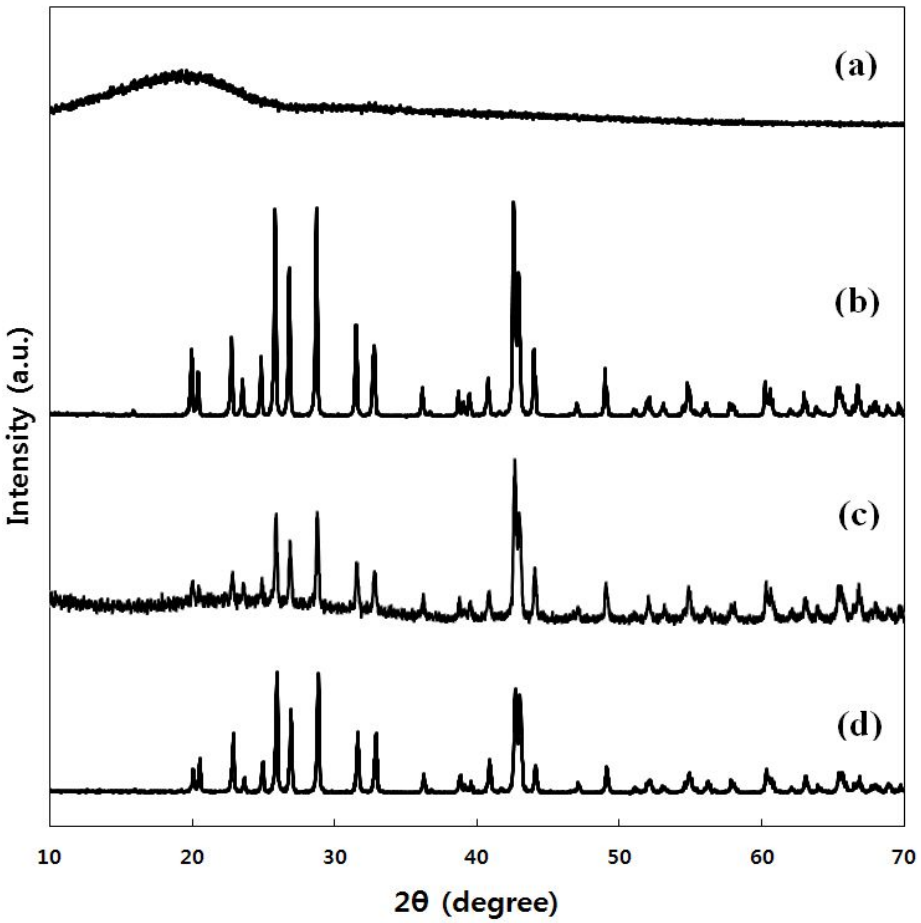

Figure 3. X-ray diffraction patterns of (a) intact PLGA powder, (b) intact $BaSO_4$ powder, (c) 3BFL and (d) 10BFL.

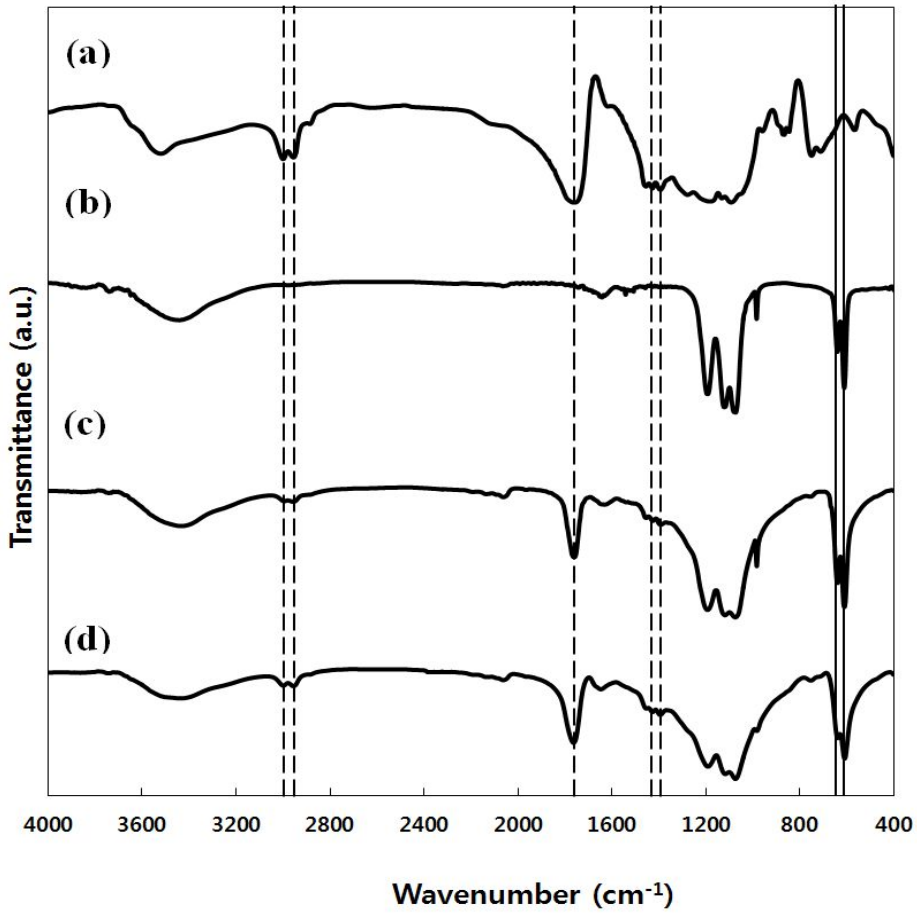

Figure 4. Fourier transform infrared spectra of (a) intact PLGA powder, (b) intact $BaSO_4$ powder, (c) 3BFL and (d) 10BFL. The solid and dashed lines indicate the major peaks from $BaSO_4$ and PLGA, respectively.

3.2. *In vitro X-ray visibility*

To examine the longevity of X-ray visibility, the radiopaque plates were immersed in a stimulated biological fluid (PBS, pH 7.4) at 37 ºC, and their X-ray images were obtained at scheduled intervals for 40 days. Figure 5(a) displays representative X-ray images of the 10BFL and 3BFL plates, both of which distinctly exhibited the radiopaque layer attached to the plate to be clearly visible throughout the testing period. As time elapsed, the square-frame shape of 3BFL became increasingly deformed, which could be a result of the swelling and degradation of the binder material, PLGA. In contrast, the shape of 10BFL did not change significantly, possibly due to the lower mass amount of PLGA incorporated into the layer ($BaSO_4$: PLGA = 10:1 w/w) and, hence, the diminished influence of the binder material. As we evaluated the images using densitometry measurements (Fig. 5 (b)), the 10BFL plate exhibited higher densitometry values than the 3BFL plate throughout the 40-day testing period due to the larger mass ratio of $BaSO_4$ in the radiopaque layer. For both radiopaque plates, the densitometry values decreased with time as the binder material increasingly swelled and degraded, causing a release and decrease in the density of the $BaSO_4$ particles.

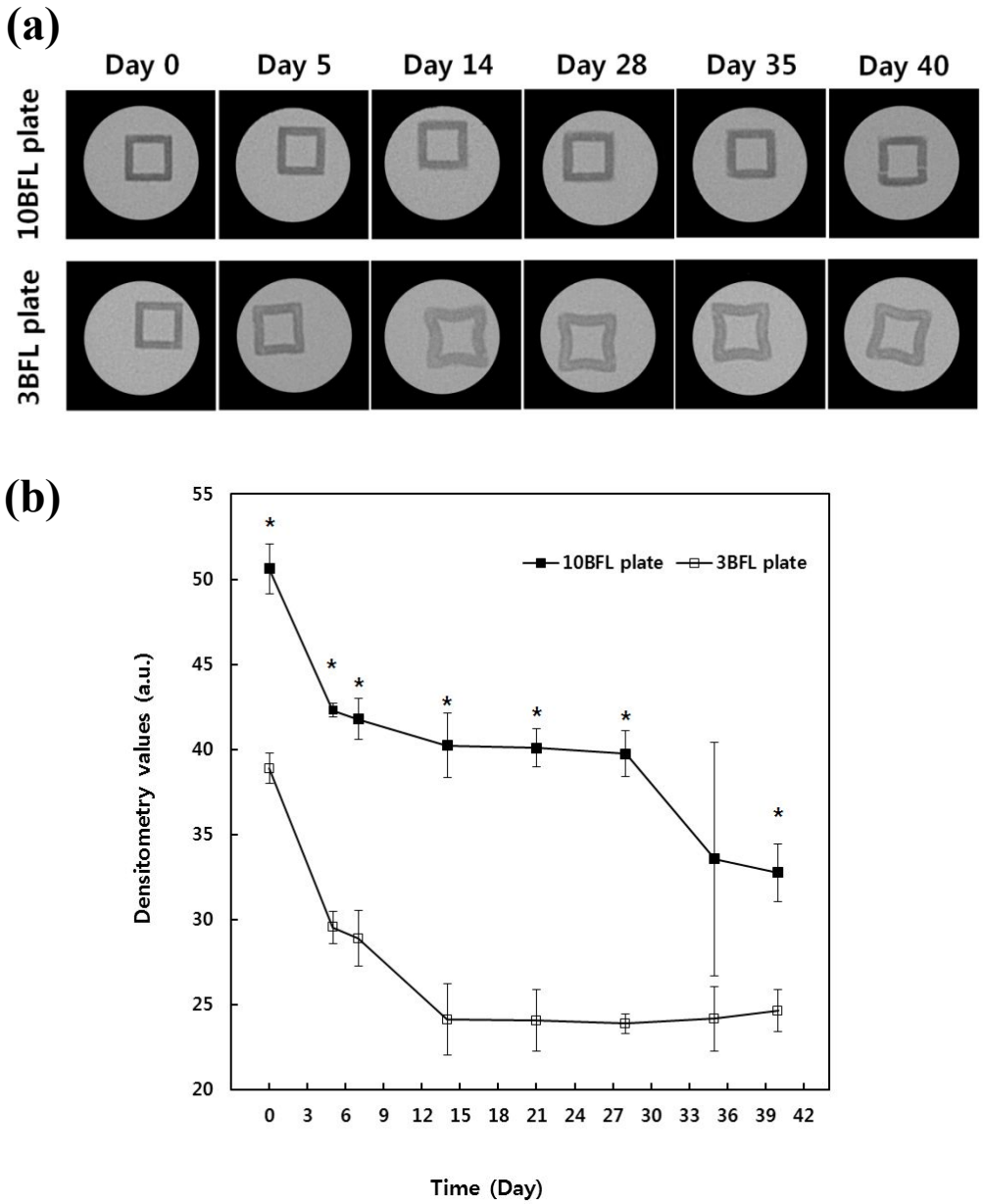

Figure 5. (a) Representative X-ray images and (b) densitometry values of the 10BFL and 3BFL plates immersed in pH 7.4 PBS at 37 ºC for 40 days. Asterisk (*) marks statistically significant difference between the 10BFL and 3BFL. ($p < 0.05$)

3.3. *Cytocompatibility of radiopaque layer*

We evaluated the cytocompatibility of the intact plate and the radiopaque plates, *i.e.*, the 10BFL and 3BFL plates. As with intact bone plate, the radiopaque layer was also designed to degrade in this work, and, thus, would release $BaSO_4$ particles. $BaSO_4$ has been reported to be toxic at elevated exposure levels [30]. However, the release of the $BaSO_4$ particles from the plates can be controlled, thereby avoiding or minimizing toxicity. With this aim, we prepared a controlled *in vitro* environment in which 2 ml of immersion medium containing the plate was fully replaced with fresh medium every two days, and the collected media were used to test cell viability.

Figure 6 displays the results from the test performed under the conditions described above. Neither the 3BFL nor 10BFL plates, nor the intact plate without a radiopaque layer, exhibited any statistically significant difference in cytotoxicity at the sampled times over 42 days when compared with the non-treated cell groups. According to the ICP measurements, $BaSO_4$ particles were indeed released (Fig. 7). However, the average $BaSO_4$ particle concentrations in the extraction media were below 0.25 mg/ml, indicating that, at most, 0.5 mg of $BaSO_4$ particles were released in each 2 ml volume of medium from each radiopaque plate every two days. This result is supported by the results of the cytotoxicity evaluation as a function of the $BaSO_4$ particle concentrations. As displayed in Figure 8, the cell viability did not appear to be affected below a 3.0 mg/ml $BaSO_4$ particle concentration.

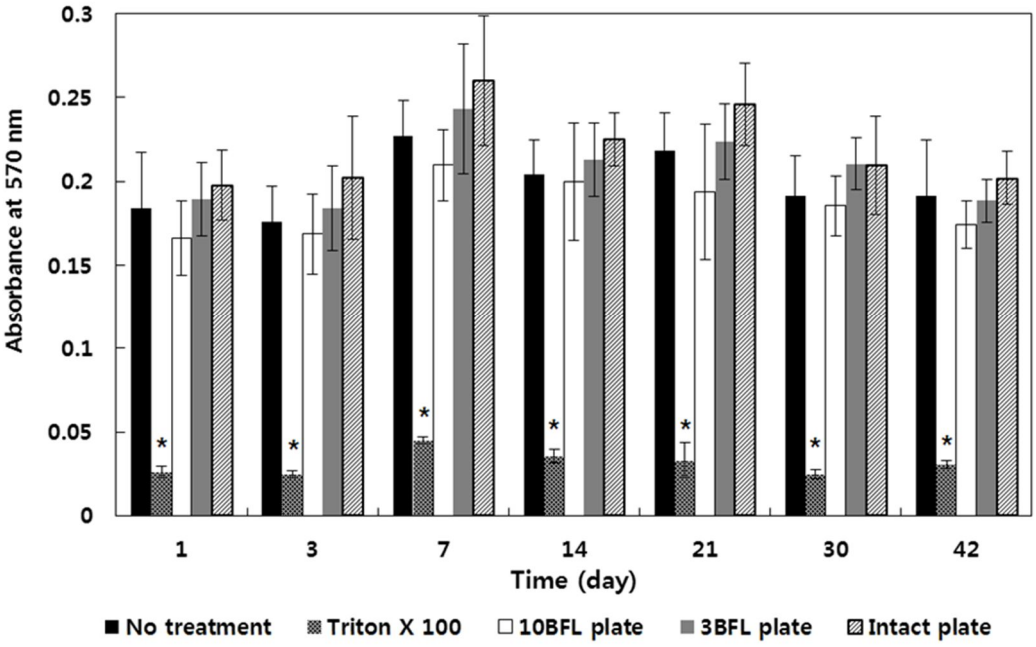

Figure 6. Cytotoxicity results evaluated by the MTT assay.

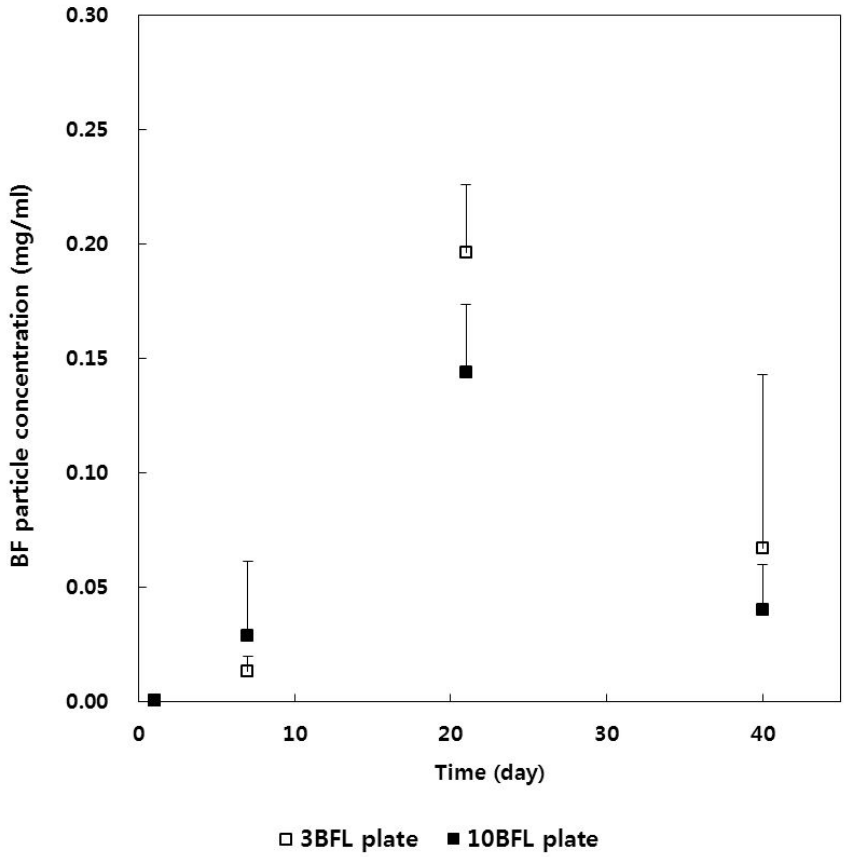

Figure 7. Concentrations of $BaSO_4$ released from the radiopaque plates. The extract media obtained on days 1, 7, 21 and 40 were then analyzed by ICP-AES.

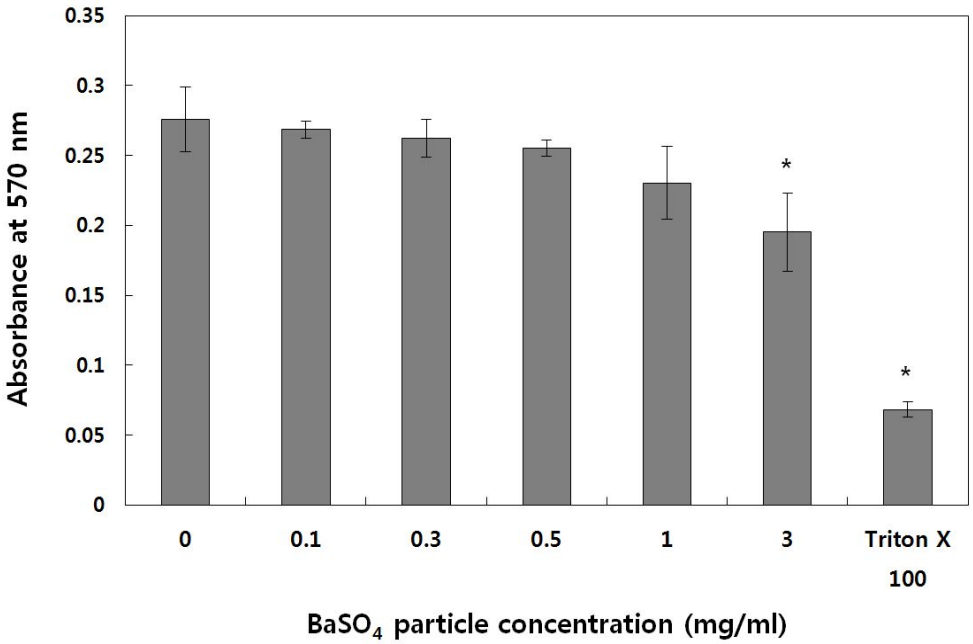

Figure 8. Cytotoxicity results evaluated by the MTT assay as a function of the $BaSO_4$ concentrations.

3.4. *In vivo X-ray visibility*

We examined the *in vivo* X-ray visibility of the radiopaque plates, 3BFL and 10BFL, for 56 days following their fixation on the rabbit humerus. As depicted in Figure 9, both radiopaque plates were discernible for the entire period of the *in vivo* experiment and showed a decrease in visibility with time, consistent with the results from the *in vitro* immersion test (Fig. 7). The PLGA incorporated into the layer caused swelling and degradation, leading to the release of $BaSO_4$ particles and affecting the X-ray visibility. According to the densitometry measurements, the 10BFL plate, *i.e.*, the plate containing more $BaSO_4$ in the radiopaque layer, exhibited better defined images than the 3BFL plate throughout the testing period of 56 days ($p < 0.05$). As we assessed the area of X-ray visibility (Fig. 9(c)), the visible area also decreased with time, again implying the gradual disappearance of the layer due to $BaSO_4$ particle release accompanied by PLGA degradation. An increase in the visible area on day 4 was ascribed to the swelling of the binder material, PLGA, immediately following implantation. During the first 45 days, the effectively visible areas were larger for the 10BFL plate due to the greater $BaSO_4$ particle content in the layer.

(a)

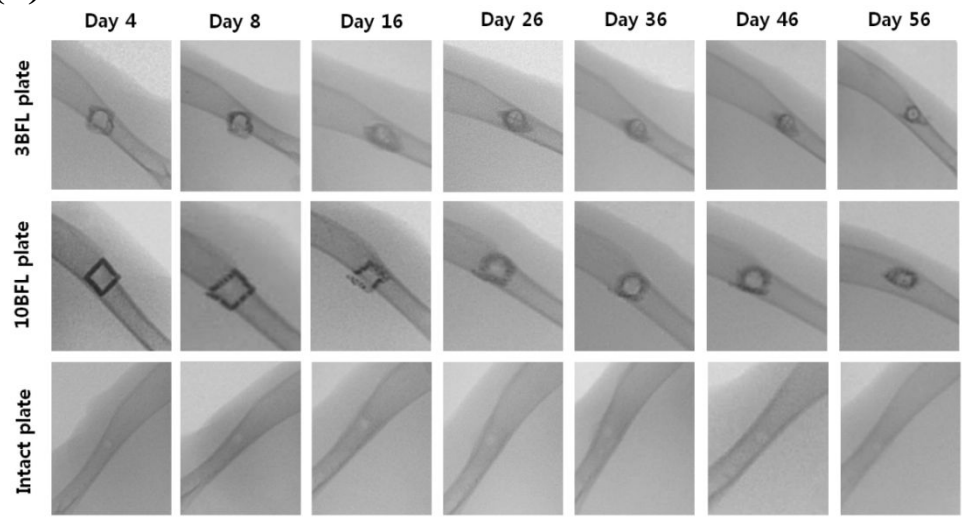
Day 4
Day 8
Day 16
Day 26
Day 36
Day 46
Day 56
3BFL plate
10BFL plate
Intact plate

(b)

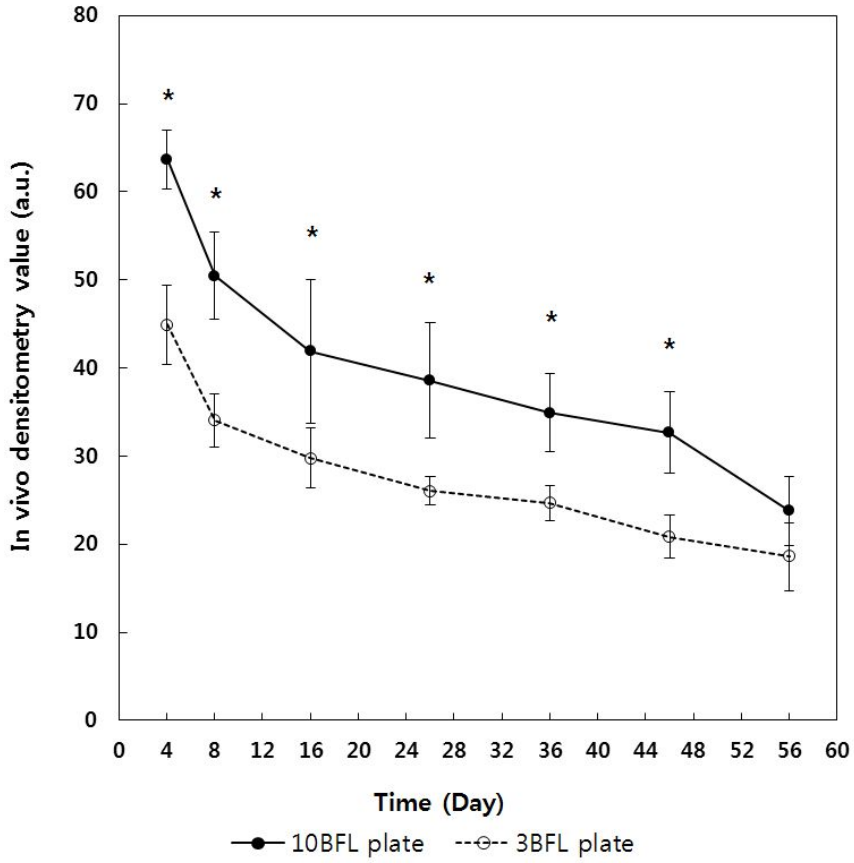
In vivo densitometry value (a.u.)
Time (Day)
10BFL plate
3BFL plate

(c)

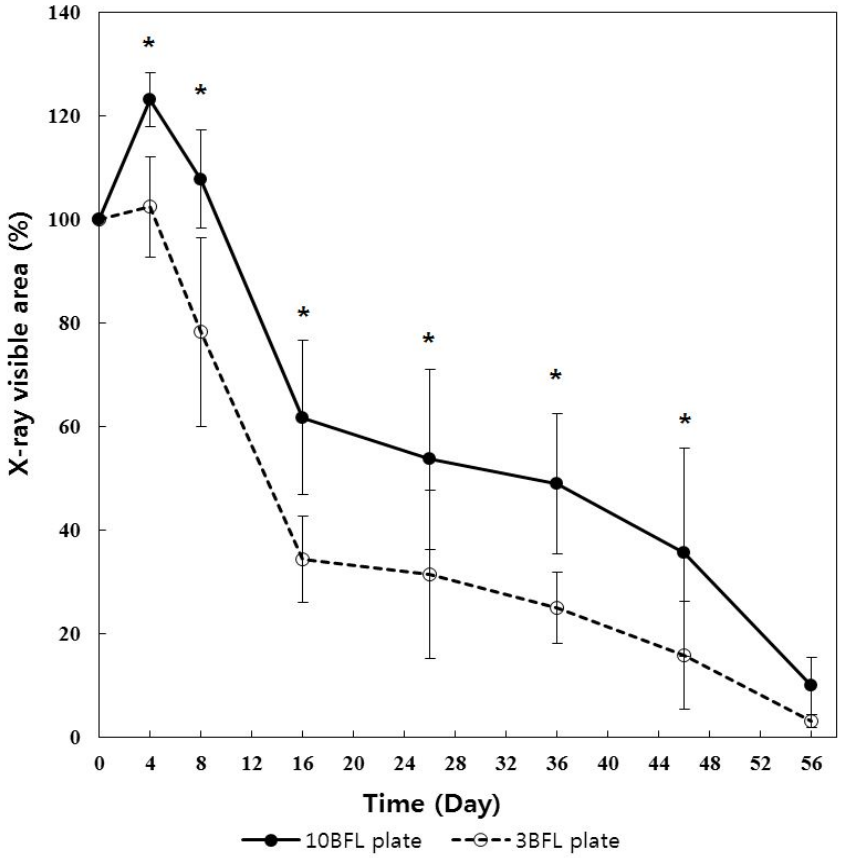

Figure 9. (a) Representative *in vivo* X-ray images from the radiopaque bone plates implanted in the rabbit. The Inion plate was also imaged for control. (b) *In vivo* densitometry measurements and (c) X-ray visible areas obtained from the radiopaque plates implanted in the rabbit *in vivo*. Asterisk (*) marks statistically significant difference between the 10BFL and 3BFL. ($p < 0.05$)

3.5. *In vivo histological analysis*

To examine the biocompatibility of the layers, we performed a histological analysis of the tissues around the radiopaque plates and compared them with the original plate in clinical use (PLT-1031, Inion, Finland) (Table A2). One week after implantation, for all of plate samples, lymphocytes had moderately infiltrated into the soft tissue surrounding the implanted screw and plate, while necrosis and abscesses were not detected and only a few neutrophils remained in the tissues (Figs. 10 and 12). However, for the 3BFL and 10BFL plates, the aggregation of pigments was observed along the surface of the plate, and some pigment-laden macrophages were detected around this area. For the 3BFL plate, giant cell infiltration was more frequent than for the 10BFL and the intact, original plates. Fibrosis with neovascularization extended into the skeletal muscle and frequently beyond the skeletal muscle for all plate samples; however, there was no discernible difference among them in the degree of fibrosis. After 4 weeks, lymphocytic infiltration was considerably resolved, and the number of pigment-laden macrophages decreased but remained with the 3BFL and 10BFL plates (Figs. 11 and 12). These results suggested that there was no apparent difference in the degree of inflammation, except in the presence of pigment laden macrophages in the radiopaque plates 4 weeks after implantation.

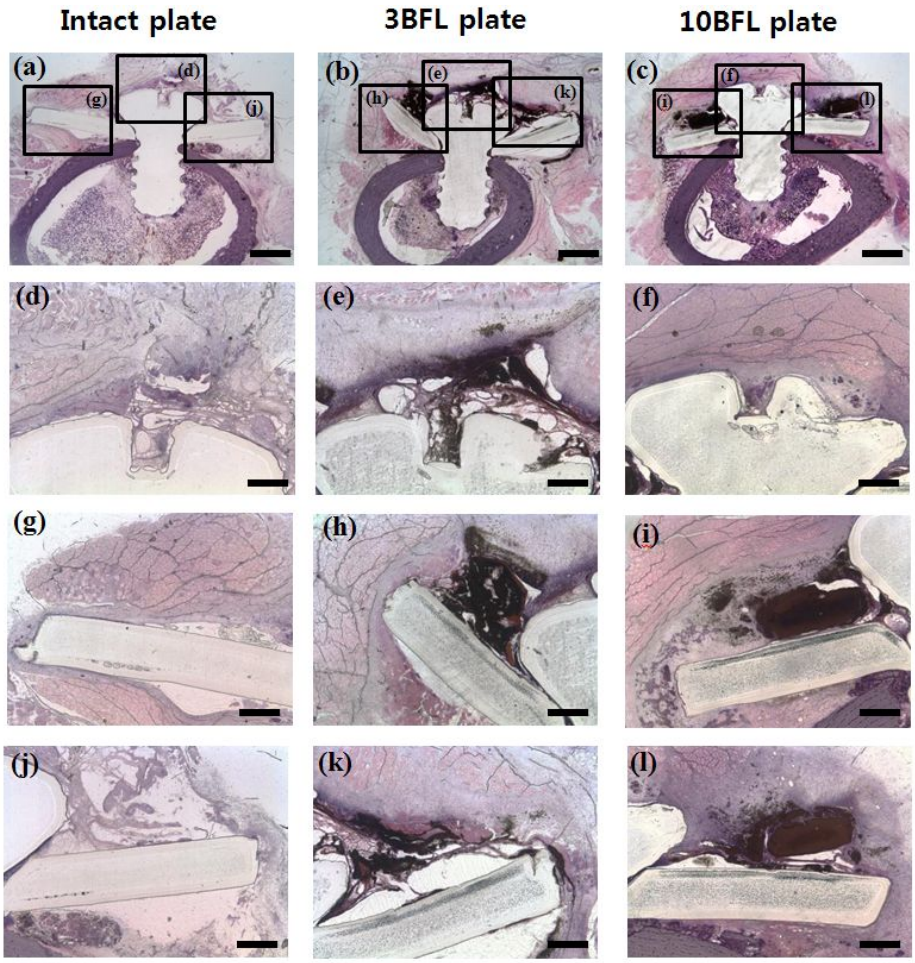

Figure 10. Histological pictures obtained from the tissue around the (a) intact Inion plate, (b) 3BFL plate and (c) 10BFL plate 1 week after implantation. The pictures of (d, g, j), (e, h, k) and (f, i, l) are from the selected areas in (a), (b) and (c), respectively, imaged at a higher magnification. The scale bars are (a-c) 300 μm and (d-l) 80 μm.

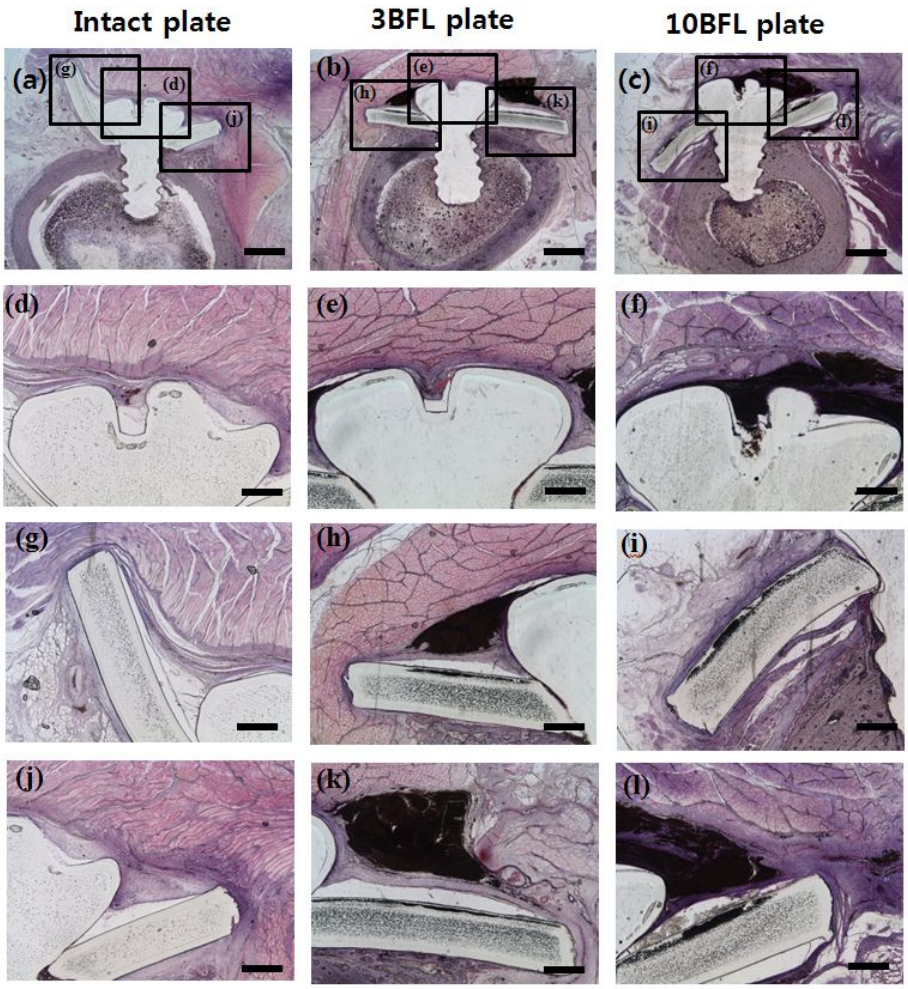

Figure 11. Histological pictures obtained from the tissue around the (a) intact Inion plate, (b) 3BFL plate and (c) 10BFL plate 4 weeks after implantation. The pictures of (d, g, j), (e, h, k) and (f, i, l) are from the selected areas in (a), (b) and (c), respectively, imaged at a higher magnification. The scale bars are (a-c) 300 μm and (d-l) 80 μm.

(a) Fibrosis

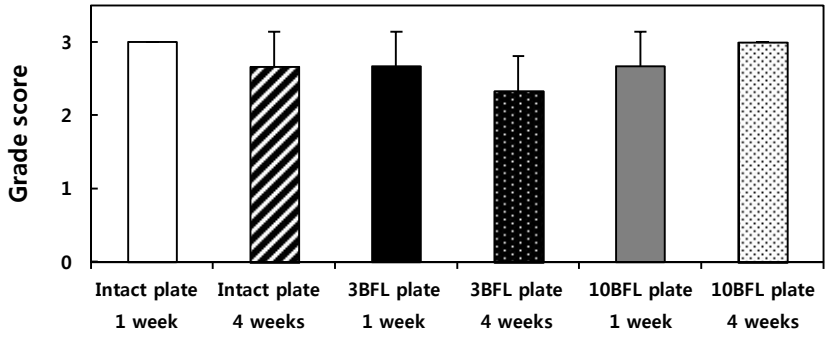

(b) New bone formation

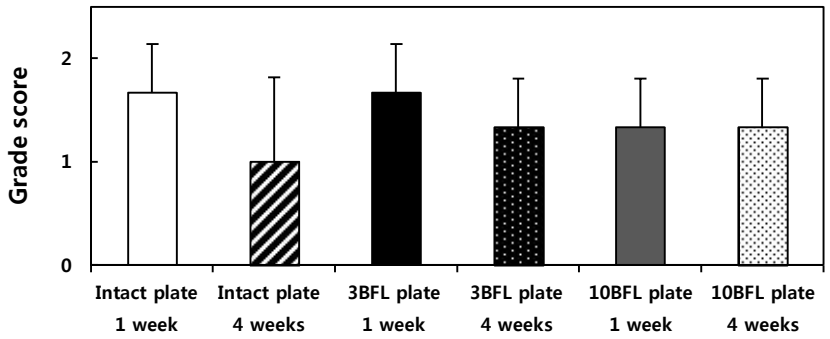

(c) Neutrophil

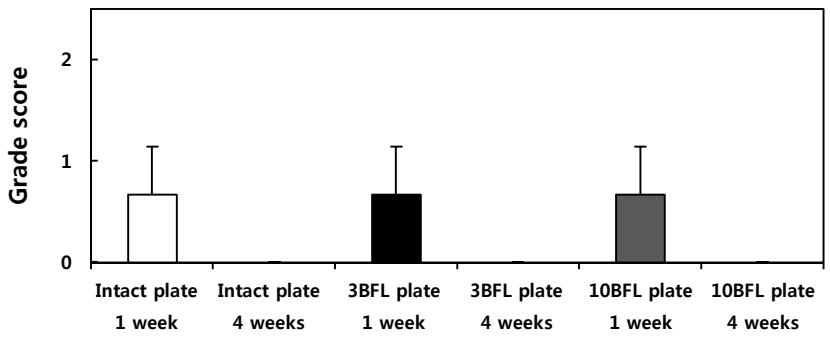

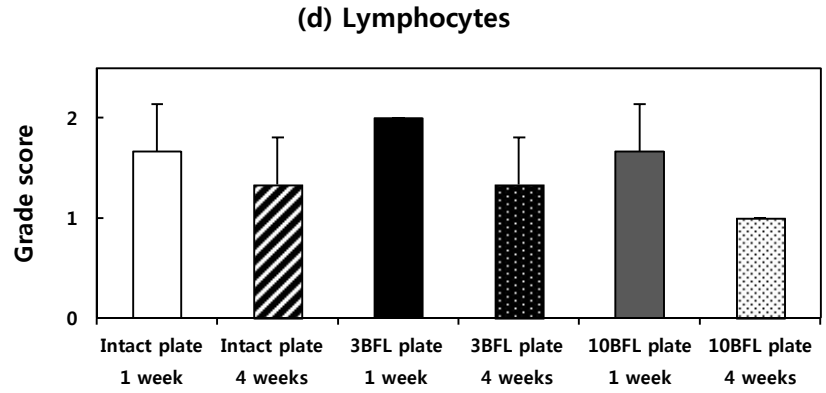

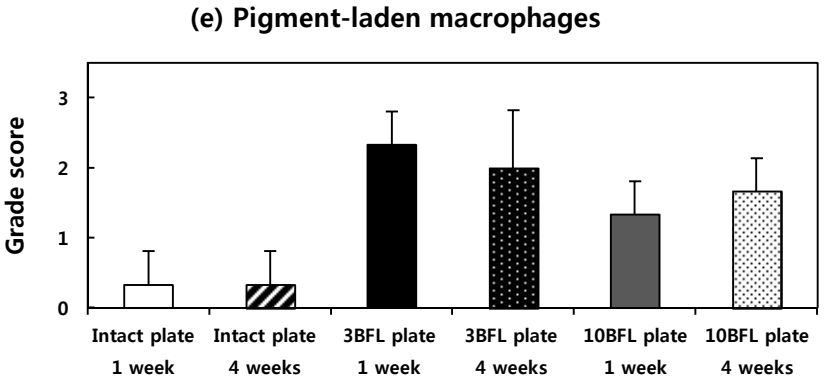

Figure 12. Histomorphometric analyses of (a) fibrosis, (b) new bone formation, (c) neutrophils, (d) lymphocytes, and (e) pigment-laden macrophages in the tissues around the intact plate, 3BFL plate and 10BFL plate 1 and 4 weeks after implantation.

Ⅳ. Discussion

Biodegradable fixation systems have been widely used in orthopedic fields for bone fracture treatment and bone reconstruction. Unlike metallic fixation systems, biodegradable systems degrade and eventually disappear in the body, thereby negating the need for a secondary removal surgery [7, 8]. However, due to the radiolucency of standard biodegradable materials, postoperative diagnosis *via* conventional X-ray imaging is limited for biodegradable fixation systems [10, 34-36]. To confer X-ray visibility, previous studies suggested the use of composites containing biodegradable polymers along with a radiopaque material to fabricate biodegradable fixation systems. However, the physical stability and mechanical strength of the plates in these studies were not satisfactory due to the radiopaque additive, limiting their utility in bone fixation [37-39].

Therefore, to confer X-ray visibility without altering the materials in the biodegradable bone plate itself, in our previous work we suggested an assembled structure of a bone plate and a radiopaque layer [25]. In this system, an X-ray visible layer composed of a radiopaque agent, β-tricalcium phosphate (TCP), and a binder material, PLGA, was independently prepared and later attached to a bone plate already in clinical use (Inion, Finland). With this approach, we were able to make the plate visible by X-ray while not significantly affecting the original, inherent properties of the bone plate itself. However, this

system required improvement: while the radiopaque plate containing TCP was visible, its resolution by X-ray imaging was not satisfactory.

In this current study, to allow improved X-ray imaging, we utilized $BaSO_4$ instead of TCP to prepare a radiopaque layer. The X-ray attenuation coefficient of barium is known to be more than 8 times larger than that of calcium [26]. Thus, when radiopaque layers were prepared under the same conditions (*i.e.*, with the same dimensions and similar quantities of radiopaque material), the layer composed of $BaSO_4$ was more clearly visible by X-ray than that of TCP (Table A1 and Fig. A1). In addition, due to its higher visibility, a thinner radiopaque layer of $BaSO_4$ could be used while maintaining good X-ray visibility. In this work, a barium sulfate ($BaSO_4$) layer of 0.5 mm thickness exhibited an average densitometry value of 50.6 (Fig. 5), approximately 7 times larger than that of a 1.3-mm thick TCP layer prepared in our previous work [25]. In terms of longevity, both the 10BFL and 3BFL plates were observable for more than 8 weeks *in vivo*, much longer than the period generally needed for the clinical diagnosis of loosening bone plates and screws [40].

Despite these advantages, a concern remained that the $BaSO_4$ in the layer would be released during PLGA degradation, resulting in toxicity at high enough exposure levels [41]. Notably, $BaSO_4$ has already been approved in clinical use as a radiopaque agent for implantable bone cement (*e.g.*, KyphX HV-R; Kyphon Inc.; USA, Simplex®P; Stryker; USA and Vertaplex; Stryker; USA), where up to 30% of the cement formulation is composed of $BaSO_4$ [42-44].

However, the $BaSO_4$ in these bone cements is designed to be contained, and have minimal $BaSO_4$ release.

In this work, we aimed to have a slow the release of $BaSO_4$ particles from the radiopaque layer in order to reduce or prevent $BaSO_4$ toxicity. A previous study reported that $BaSO_4$ concentrations above a certain threshold caused cytotoxicity [28]. In this work, the radiopaque layers were designed to slowly decompose concurrently with the original, intact Inion bone plate. Importantly, the radiopaque layers (*i.e.*, 10BFL and 3BFL) released the $BaSO_4$ particles slowly, at a rate of less than 0.5 mg per day (Fig. 7). Thus, when tested under a controlled *in vitro* environment, where the *in vivo* clearance of the $BaSO_4$ particles was assumed, the radiopaque plates did not exhibit significant cytotoxicity (Fig. 6). When we evaluated the biocompatibility *in vivo*, the 10BFL and 3BFL plates did not exhibit significant toxicity, and the inflammatory responses were similar to those of the Inion plates already in clinical use (Figs. 10 and 11).

Ⅴ. Conclusion

Due to their radiolucent properties, biodegradable bone fixation devices present challenges in X-ray imaging, which is often needed to monitor their proper positioning after fixation. To enable X-ray visibility, we developed an assembled structure of a bone plate in clinical use (Inion, Finland) and a radiopaque layer, which was composed of barium sulfate and PLGA as radiopaque and binder materials, respectively. The degree of X-ray visibility could be varied depending on the mass ratio of $BaSO_4$ in the layer, and the layer could be tailored to degrade and disappear gradually along with the original Inion plate. In this work, the X-ray image from the 10BFL plate was more discernible than that from the 3BFL plate because it contained a greater amount of $BaSO_4$ in the radiopaque layer. Due to the presence of the binder material, PLGA, the X-ray visibility decreased with time, although the plates remained observable for up to 56 days *in vivo*. The release of $BaSO_4$ particles during layer degradation can be controlled to avoid or minimize possible toxicity. The radiopaque plates in this work were observed to release less than 0.5 mg of $BaSO_4$ particles every two days, which was insufficient to induce cytotoxicity when tested under a controlled *in vitro* environment. According to the *in vivo* experiments with rabbits, the radiopaque plates exhibited good biocompatibility, similar to that of the Inion plate already in clinical use. Therefore, we concluded that a biodegradable bone plate assembled with a $BaSO_4$-based, radiopaque

layer has the potential to be used as an orthopedic fixation system to enable X-ray imaging diagnosis.

Ⅵ. References

1. Malekani, J., et al. *Biomaterials in orthopedic bone plates: a review.* in *Proceedings of the 2nd Annual International Conference on Materials Science, Metal & Manufacturing (M3 2011)*. 2011. Global Science and Technology Forum.
2. Goodrich, J.T., A.L. Sandler, and O. Tepper, *A review of reconstructive materials for use in craniofacial surgery bone fixation materials, bone substitutes, and distractors.* Child's Nervous System, 2012. **28**(9): p. 1577-1588.
3. Hintermann, B., H. Trouillier, and D. Schäfer, *Rigid internal fixation of fractures of the proximal humerus in older patients.* Journal of Bone & Joint Surgery, British Volume, 2000. **82**(8): p. 1107-1112.
4. Uhthoff, H.K., P. Poitras, and D.S. Backman, *Internal plate fixation of fractures: short history and recent developments.* Journal of Orthopaedic Science, 2006. **11**(2): p. 118-126.
5. Voggenreiter, G., et al., *Immuno-inflammatory tissue reaction to stainless-steel and titanium plates used for internal fixation of long bones.* Biomaterials, 2003. **24**(2): p. 247-254.
6. Lee, J.H. and J.H. Park, *The Clinical Usefulness of Ultrasound-Aided Fixation Using an Absorbable Plate System in Patients*

with Zygomatico-Maxillary Fracture. Archives of plastic surgery, 2013. **40**(4): p. 330-334.

7. Richards, R., J. Palmer, and N. Clarke, *Observations on removal of metal implants.* Injury, 1992. **23**(1): p. 25-28.
8. Rokkanen, P.U., et al., *Bioabsorbable fixation in orthopaedic surgery and traumatology.* Biomaterials, 2000. **21**(24): p. 2607-2613.
9. Ambrose, C.G. and T.O. Clanton, *Bioabsorbable implants: review of clinical experience in orthopedic surgery.* Annals of biomedical engineering, 2004. **32**(1): p. 171-177.
10. Chaushu, G., et al., *Risk factors contributing to symptomatic plate removal in maxillofacial trauma patients.* Plastic and reconstructive surgery, 2000. **105**(2): p. 521-525.
11. Daniels, A., et al., *Mechanical properties of biodegradable polymers and composites proposed for internal fixation of bone.* Journal of applied biomaterials, 1990. **1**(1): p. 57-78.
12. H. Wolfgang Losken, J.A.v.A., Mark P. Mooney, Virginia L. Godfrey, Tripti Burt, Sumeet Teotia, Shay B. Dean, Jonathan R. Moss, Reza Rahbar, *Biodegradation of Inion Fast-Absorbing Biodegradable Plates and Screws.* The journal of craniofacial surgery, 2008. **19**.

13. Ikada, Y., et al., *Enhancement of bone formation by drawn poly (L-lactide).* Journal of biomedical materials research, 1996. **30**(4): p. 553-558.

14. Athanasiou, K.A., et al., *Orthopaedic applications for PLA-PGA biodegradable polymers.* Arthroscopy: The Journal of Arthroscopic & Related Surgery, 1998. **14**(7): p. 726-737.

15. Tokiwa, Y. and B.P. Calabia, *Biodegradability and biodegradation of poly (lactide).* Applied microbiology and biotechnology, 2006. **72**(2): p. 244-251.

16. Böstman, O.M. and H.K. Pihlajamäki, *Adverse tissue reactions to bioabsorbable fixation devices.* Clin Orthop Relat Res, 2000. **371**: p. 216-227.

17. Mainil-Varlet, P., B. Rahn, and S. Gogolewski, *Long-term in vivo degradation and bone reaction to various polylactides. 1. One-year results.* Biomaterials, 1997. **18**(3): p. 257-66.

18. Middleton, J.C. and A.J. Tipton, *Synthetic biodegradable polymers as orthopedic devices.* Biomaterials, 2000. **21**(23): p. 2335-2346.

19. Fouad, H., *Effects of the bone-plate material and the presence of a gap between the fractured bone and plate on the predicted*

stresses at the fractured bone. Medical engineering & physics, 2010. **32**(7): p. 783-789.

20. Blokhuis, T., et al., *The reliability of plain radiography in experimental fracture healing.* Skeletal radiology, 2001. **30**(3): p. 151-156.

21. Gefen, A., *Optimizing the biomechanical compatibility of orthopedic screws for bone fracture fixation.* Medical engineering & physics, 2002. **24**(5): p. 337-347.

22. Hume, M.C. and D.A. Wiss, *A clinical and radiographic comparison of tension band wiring and plate fixation.* Clin Orthop Relat Res, 1992. **285**: p. 229-235.

23. Sanger, C., et al., *Maximizing results in craniofacial surgery with bioresorbable fixation devices.* Journal of Craniofacial Surgery, 2007. **18**(4): p. 926-930.

24. Waris, E., et al., *Self-reinforced bioabsorbable miniplates for skeletal fixation in complex hand injury: three case reports.* The Journal of hand surgery, 2004. **29**(3): p. 452-457.

25. Shasteen, C., et al., *Biodegradable internal fixation plates enabled with X-ray visibility by a radiopaque layer of β-tricalcium phosphate and poly (lactic-co-glycolic acid).* Journal

of Biomedical Materials Research Part B: Applied Biomaterials, 2013. **101**(2): p. 320-329.

26. Hubbell, J.H. and S.M. Seltzer, *Tables of X-ray mass attenuation coefficients and mass energy-absorption coefficients 1 keV to 20 MeV for elements Z= 1 to 92 and 48 additional substances of dosimetric interest*, 1995, National Inst. of Standards and Technology-PL, Gaithersburg, MD (United States). Ionizing Radiation Div.

27. Nuutinen, J.-P., C. Clerc, and P. Törmälä, *Mechanical properties and in vitro degradation of self-reinforced radiopaque bioresorbable polylactide fibres.* Journal of Biomaterials Science, Polymer Edition, 2003. **14**(7): p. 665-676.

28. Pepiol, A., et al., *A highly radiopaque vertebroplasty cement using tetraiodinated o-carborane additive.* Biomaterials, 2011. **32**(27): p. 6389-6398.

29. Lieberman, I.H., D. Togawa, and M.M. Kayanja, *Vertebroplasty and kyphoplasty: filler materials.* The Spine Journal, 2005. **5**(6): p. S305-S316.

30. Mottu, F., D.A. RüFENACHT, and E. Doelker, *Radiopaque polymeric materials for medical applications: Current aspects*

of biomaterial research. Investigative radiology, 1999. **34**(5): p. 323.

31. Iso, E., *10993-5: Biological evaluation of medical devices.* Tests for in vitro cytotoxicity, 1999.

32. Zhang, M., et al., *Synthesis and surface properties of submicron barium sulfate particles.* Applied Surface Science, 2011. **258**(1): p. 24-29.

33. Xin, F., et al., *Effects of surface modification on the properties of poly (lactide-co-glycolide) composite materials.* Polymer-Plastics Technology and Engineering, 2009. **48**(6): p. 658-664.

34. Shikinami, Y. and M. Okuno, *Bioresorbable devices made of forged composites of hydroxyapatite (HA) particles and poly L-lactide (PLLA). Part II: practical properties of miniscrews and miniplates.* Biomaterials, 2001. **22**(23): p. 3197-3211.

35. Böstman, O. and H. Pihlajamäki, *Clinical biocompatibility of biodegradable orthopaedic implants for internal fixation: a review.* Biomaterials, 2000. **21**(24): p. 2615-2621.

36. Chan, W., et al., *Effect of radio-opaque filler on biodegradable stent properties.* Journal of Biomedical Materials Research Part A, 2006. **79**(1): p. 47-52.

37. Nottelet, B., J. Coudane, and M. Vert, *Synthesis of an X-ray opaque biodegradable copolyester by chemical modification of poly (ε-caprolactone)*. Biomaterials, 2006. **27**(28): p. 4948-4954.

38. Furukawa, T., et al., *Histomorphometric study on high-strength hydroxyapatite/poly (L-lactide) composite rods for internal fixation of bone fractures.* Journal of biomedical materials research, 2000. **50**(3): p. 410-419.

39. Aldenhoff, Y.B., et al., *Stability of radiopaque iodine-containing biomaterials.* Biomaterials, 2002. **23**(3): p. 881-886.

40. Coletti, D.P., A. Salama, and J.F. Caccamese Jr, *Application of intermaxillary fixation screws in maxillofacial trauma.* Journal of Oral and Maxillofacial Surgery, 2007. **65**(9): p. 1746-1750.

41. Wimhurst, J., R. Brooks, and N. Rushton, *The effects of particulate bone cements at the bone-implant interface.* Journal of Bone & Joint Surgery, British Volume, 2001. **83**(4): p. 588-592.

42. Kjellson, F., et al., *Bone cement X-ray contrast media: A clinically relevant method of measuring their efficacy.* Journal of Biomedical Materials Research Part B: Applied Biomaterials, 2004. **70**(2): p. 354-361.

43. Kühn, K., *Bone cements. Up-to-date comparison of physical and chemical properties of commercial materials. 2000*, Springer-Verlag, Berlin.

44. Lewis, G., *Injectable bone cements for use in vertebroplasty and kyphoplasty: State-of-the-art review.* Journal of Biomedical Materials Research Part B: Applied Biomaterials, 2006. **76**(2): p. 456-468.

Ⅶ. Appendix

X-ray visible properties of TCP- and $BaSO_4$-based radiopaque layers

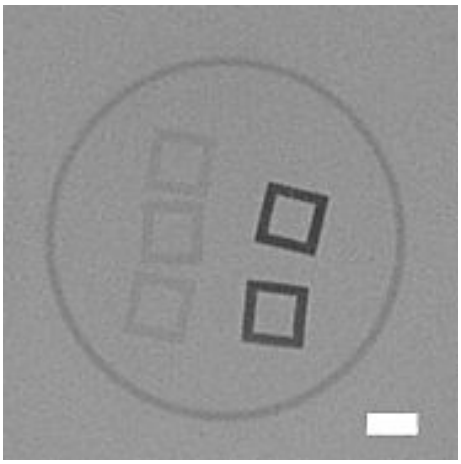

Figure A1. The X-ray images of the bioabsorbable fixation plates attached with a radiopaque layer. The three on the left contain β-tricalcium phosphate (TCP), and the two on the right contain barium sulfate ($BaSO_4$). All layers were 0.5 mm in thickness and contained similar amounts of a radiopaque material (18.62 ± 0.44 mg TCP or 25.60 ± 1.27 mg $BaSO_4$). The radiopaque layers were imaged with a mobile C-arm (BV pulsera, Philips, Netherlands) in manual mode with a charging voltage of 55 kV. The scale bar = 500 μm.

	Barium sulfate layers	**β-tricalcium phosphate layers**
Densitometry value	**59.02 ± 0.014**	**6.81 ± 0.002**

Table A1. Densitometry values obtained from the X-ray image in Figure A1.

Details for Semi-quantitative Histological Analysis

	Intact plate			
	Section 1	Section 2	Section 3	Mean ± SD
1 week after operation				
Fibrosis	3	3	3	3.00 ± 0.00
New bone formation	2	1	2	1.67 ± 0.47
Neutrophil	1	0	1	0.67 ± 0.47
Abscess	0	0	0	0.00 ± 0.00
Lymphocytes	2	2	1	1.67 ± 0.47
Pigment-laden macrophages	1	0	0	0.33 ± 0.47
4 weeks after operation				
Fibrosis	3	2	3	2.67 ± 0.47
New bone formation	1	2	0	1.00 ± 0.82
Neutrophil	0	0	0	0.00 ± 0.00
Abscess	0	0	0	0.00 ± 0.00
Lymphocytes	2	1	1	1.33 ± 0.47
Pigment-laden macrophages	1	0	0	0.33 ± 0.47
	3 BFL plate			
	Section 1	Section 2	Section 3	Mean ± SD
1 week after operation				
Fibrosis	3	2	3	2.67 ± 0.47
New bone formation	2	1	2	1.67 ± 0.47
Neutrophil	1	0	1	0.67 ± 0.47
Abscess	0	0	0	0.00 ± 0.00
Lymphocytes	2	2	2	2.00 ± 0.00
Pigment-laden macrophages	2	2	3	2.33 ± 0.47
4 weeks after operation				
Fibrosis	3	2	2	2.33 ± 0.47
New bone formation	1	2	1	1.33 ± 0.47
Neutrophil	0	0	0	0.00 ± 0.00
abscess	0	0	0	0.00 ± 0.00
lymphocytes	2	1	1	1.33 ± 0.47
pigment-laden macrophages	3	2	2	2.33 ± 0.47

	10BFL plate			
	Section 1	Section 2	Section 3	Mean ± SD
1 week after operation				
Fibrosis	2	3	3	2.67 ± 0.47
New bone formation	2	1	1	1.33 ± 0.47
Neutrophil	1	1	0	0.67 ± 0.47
Abscess	0	0	0	0.00 ± 0.00
Lymphocytes	2	2	1	1.67 ± 0.47
Pigment-laden macrophages	2	1	1	1.33 ± 0.47
4 weeks after operation				
Fibrosis	3	3	3	3.00 ± 0.00
New bone formation	2	1	1	1.33 ± 0.47
Neutrophil	0	0	0	0.00 ± 0.00
Abscess	0	0	0	0.00 ± 0.00
Lymphocytes	1	1	1	1.00 ± 0.00
Pigment-laden macrophages	2	1	2	1.67 ± 0.47

Table A2. Semi-quantitative histological analysis to evaluate tissue reaction 1 and 4 weeks after implantation.

국문초록

진단용 X-선 영상을 위한 황산바륨 조영층이 결합된 생체흡수성 골 고정용 플레이트의 개발

골절된 뼈의 고정을 위해 사용되는 금속합금 기반의 플레이트는 높은 기계적 강도의 장점으로 널리 이용되고 있지만, 간혹 금속재료의 부식물에 대한 독성문제, 골절 치유 이후 2 차 제거수술에 대한 환자의 부담감 및 플레이트 자체의 뼈보다 높은 강도로 인하여 접합된 뼈의 강도가 낮아지게 되는 문제점을 보유하고 있다. 이에 반하여, 흡수성 고분자재료 기반의 골 고정용 플레이트는 시술 후 생 분해되어 사라지는 재료의 특성으로 2 차 제거수술이 필요하지 않고 분해되는 과정 중에 자체적으로 줄어드는 강도의 특성을 통하여 치유된 뼈의 강도를 높이는 기능을 지니고 있다. 하지만 고분자 재료 자체의 X-ray 투과성으로 인하여 골절 수술 후에 X-선 영상을 통해 시술 후 진단에 필수적인 플레이트의 위치를 파악하기 어렵다는 단점을 지니고 있다. 이를 해결하고자, 본 연구에서는 조영 역할을 하는 황산바륨과 생분해성 폴리(락틱-코-글리콜산) (PLGA) 고분자의 혼합물을 이용하여 진단 층을 별도로 제작하여 기 허가된 흡수성 플레이트 위에 부착함으로써 X-ray 진단을 가능케 하였다. 조영층의 PLGA 고분자와 황산바륨 조영제 조성을 1:10(w/w)과 1:3(w/w)으로 구성하여, 조영능 유지기간 동안 방출되는

황산바륨입자에 대한 독성을 조절하고자 하였다. 세포독성실험을 통하여 조영능 유지기간 동안 방출되는 황산바륨입자에 대한 세포독성이 심각하지 않음을 알 수 있었다. 또한 토끼를 이용한 동물실험을 통하여 조영능 유지기간 동안 조직학적으로 생체적합함을 증명하였고, 조영층은 시간이 지남에 따라 PLGA 고분자의 분해에 의해 점차 사라지며 조영능이 감소하는 것을 확인하였다. 따라서 본 연구에서는 조영층이 결합된 생체흡수성 골고정용 플레이트가 수술 후 고정 장치의 위치를 쉽게 파악할 수 있는 X-선 진단이 가능한 생체흡수성 골고정용 플레이트를 제작하여 진단 및 치료의 복합적 기능을 갖춘 골고정용 시스템에의 응용 가능성을 고찰해 보았다.

주 요 어 : 황산바륨, 생체적합성, 생분해성, 골 고정 시스템, 폴리(락틱-코-글리콜산), X-선 조영.

학 번 : 2012-21022

감사의 글

본 졸업논문을 위해 유익한 말씀과 충고로 정성껏 지도해 주신 최영빈 교수님께 감사 드립니다. 또한, 바쁘신 중에도 논문심사를 맡아주신 김희찬 교수님, 김성완 교수님께도 감사 드립니다.

그리고 이 연구를 위하여 동물실험과 조직평가에 있어 아낌없는 조언과 격려를 해주신 최태현 교수님과 민혜숙 교수님 그리고 연구원들에게 감사의 말씀을 전합니다. 더불어 학문적으로 그리고 인생의 좋은 동료였던 BPAL 연구실 선후배님께 감사의 마음을 전합니다.

마지막으로 연구에 몰두할 수 있도록 아낌없는 지원을 해주신 부모님과 항상 든든한 지원군인 언니에게 감사의 인사를 전합니다. 행복한 가정에서 자랄 수 있게 해주심에 깊이 감사 드리고, 언제나 옳은 선택을 하도록 기도를 해주신 덕분에 무사히 석사 졸업을 할 수 있었습니다. 고맙습니다.

이 글에 모두 싣지 못한 많은 분들의 도움으로 석사졸업을 하며, 이러한 도움에 보답하는 마음으로 앞으로도 최선을 다하겠습니다. 감사합니다.

본 연구는 보건복지부 보건의료연구개발사업의 지원을 받아 수행되었습니다. (과제고유번호: A110962)